Localization in band random matrix models with and without increasing diagonal elements

Wen-ge Wang
Department of Physics, Southeast University, Nanjing 210096, China
and Department of Physics, National University of Singapore, 119260, Singapore
(Received 10 December 2001; published 19 June 2002)

It is shown that localization of eigenfunctions in the Wigner band random matrix model with increasing diagonal elements can be related to localization in a band random matrix model with random diagonal elements. The relation is obtained by making use of a result of a generalization of Brillouin-Wigner perturbation theory, which shows that reduced Hamiltonian matrices with relatively small dimensions can be introduced for nonperturbative parts of eigenfunctions, and by employing intermediate basis states, which can improve the method of the reduced Hamiltonian matrix. The latter model deviates from the standard band random matrix model mainly in two aspects: (i) the root mean square of diagonal elements is larger than that of off-diagonal elements within the band, and (ii) statistical distributions of the matrix elements are close to the Lévy distribution in their central parts, except in the high top regions.

DOI: 10.1103/PhysRevE.65.066207 PACS number(s): 05.45.−a

I. INTRODUCTION

One of the most important discoveries in the field of quantum chaos is dynamical localization in time-dependent systems [1]. Recently, a similar phenomenon has also been found in conservative systems [2–6]. Among them, the simplest model employed is the so-called Wigner band random matrix (WBRM) model [2], consisting of matrices with increasing diagonal elements and random off-diagonal elements within a band, which was introduced in the study of complex systems, such as complex nuclei [7] and complex atoms [8]. Even for such a simple model, the mechanism of localization is still unclear. Unlike the average shape of the so-called local spectral density of states in the model, which can be established analytically [9], the properties of eigenfunctions have been determined mainly numerically. Making use of a so-called generalization of Brillouin-Wigner perturbation theory (GBWPT) [10], which separates energy eigenfunctions into perturbative (PT) and nonperturbative (NPT) parts, localization in the WBRM model has been found to appear in fact in NPT parts of eigenfunctions [11]. Since the present form of the GBWPT supplies quite limited information on properties of NPT parts of eigenfunctions, an explanation for localization in them is still absent.

A possible way of deepening the understanding of localization in the WBRM model is to relate it to localization in some other models, similar to the case for the model of the kicked rotator on the torus and the one-dimensional tight-binding model [12]. For example, one may consider the standard band random matrix (BRM) model, the theory of which has been well developed (see, e.g., [13–17]). The main difference between the two models is that the former has increasing diagonal elements and the latter has random diagonal elements. However, in view of the GBWPT, the difference is not so large when only the NPT parts of eigenfunctions are of interest, since the numbers of components in them are usually smaller than the dimension of the random matrices. In fact, the central parts of the eigenfunctions in the WBRM model have been found possibly lying in any region of their NPT parts, which suggests that diagonal elements do not dominate in the determination of the positions of the central parts in the corresponding NPT regions of the eigenfunctions.

In this paper, we shall show that the analytical expression for the PT parts of the eigenfunctions in the GBWPT can be made use of in investigation of the properties of the corresponding NPT parts. For each eigenfunction of a perturbed Hamiltonian, one can introduce a reduced Hamiltonian matrix which has an eigenfunction possessing the same components as the NPT part of the eigenfunction. A direct application of the method of reduced Hamiltonian matrices to the WBRM model gives no insight into the mechanism of localization in it, since such matrices still have increasing diagonal elements. To solve this problem, we will convert the original basis states to some intermediate basis states, in which the sizes of the NPT parts of the eigenfunctions are much reduced and the diagonal elements of the reduced Hamiltonian matrices fluctuate around their mean values. Then it becomes possible to relate localization in the WBRM model to some BRM model with random diagonal elements, which is in fact close to a so-called superimposed BRM (SBRM) model introduced and investigated in Ref. [18].

The paper is organized as follows. In Sec. II, the reduced Hamiltonian matrices are introduced. Section III is devoted to an investigation of properties of the WBRM model in the intermediate basis states. In particular, the reduced Hamiltonian matrices are shown to be related to a BRM model, in which it is reasonable to expect localization to appear. It is shown that, if the eigenfunctions of the reduced Hamiltonian matrices in intermediate basis states are localized, the eigenfunctions of the WBRM model in the original basis states should be localized as well. Conclusions and discussion are given in Sec. IV.

II. REDUCED HAMILTONIAN MATRICES FOR NONPERTURBATIVE PARTS OF EIGENSTATES

Consider a Hamiltonian of the form $H=H_0+V$, where H_0 is an unperturbed Hamiltonian and V represents a perturbation. The eigenstates of the Hamiltonians H and H_0 are

denoted by $|\alpha\rangle$ and $|k\rangle$, respectively,

$$H|\alpha\rangle = E_\alpha|\alpha\rangle, \quad H_0|k\rangle = E_k^0|k\rangle, \tag{1}$$

with the labels $\alpha, k = 1,2,\ldots$ and α in energy order. Here, the perturbation V is assumed to have zero diagonal elements in the H^0 representation. (Nonzero diagonal elements of V, if there are any, can be attributed to H_0.) Components of $|\alpha\rangle$ in $|k\rangle$ are denoted as $C_{\alpha k} = \langle k|\alpha\rangle$. In the GBWPT, for each perturbed state $|\alpha\rangle$, the set of unperturbed states $|k\rangle$ is divided into two subsets, denoted by S_α and $\overline{S}_\alpha$, and consequently the perturbed state itself is divided into two parts, $|\alpha_s\rangle \equiv P_{S_\alpha}|\alpha\rangle$ and $|\alpha_{\bar{s}}\rangle \equiv Q_{\overline{S}_\alpha}|\alpha\rangle$, respectively, by two projection operators

$$P_{S_\alpha} = \sum_{|k\rangle \in S_\alpha} |k\rangle\langle k|, \quad Q_{\overline{S}_\alpha} = \sum_{|k\rangle \in \overline{S}_\alpha} |k\rangle\langle k| = 1 - P_{S_\alpha}. \tag{2}$$

When the condition

$$\lim_{n\to\infty} \langle\alpha|(T_\alpha^\dagger)^n T_\alpha^n|\alpha\rangle = 0 \tag{3}$$

is satisfied, where $T_\alpha = [1/(E_\alpha - H_0)]Q_{\overline{S}_\alpha}V$, it can be shown rigorously [10] that the part $|\alpha_{\bar{S}}\rangle$ can be expanded in a convergent perturbation expansion,

$$|\alpha_{\bar{S}}\rangle = T_\alpha|\alpha_s\rangle + T_\alpha^2|\alpha_s\rangle + \cdots + T_\alpha^n|\alpha_s\rangle + \cdots. \tag{4}$$

For an unperturbed state $|j\rangle$ belonging to the set $\overline{S}_\alpha$, $C_{\alpha j} = \langle j|\alpha_{\bar{S}}\rangle$ can be expressed in a form making use of the concept of a path [10]. To define a path, consider $q-1$ unperturbed states $|k_l\rangle$ $(l = 1,\ldots,q-1)$ in $\overline{S}_\alpha$ and two unperturbed states $|k_0\rangle$ and $|k_q\rangle$ in either S_α or $\overline{S}_\alpha$. The sequence $k_0 \to k_1 \to \cdots \to k_{q-1} \to k_q$ is termed *a path of q paces from* k_0 *to* k_q, denoted by s, if the direct coupling $V_{k_l,k_{l+1}} = \langle k_l|V|k_{l+1}\rangle$ is nonzero for each pace. To each pace $k_l \to k_{l+1}$, we attribute a factor $D_\alpha(k_l \to k_{l+1})$, defined by $D_\alpha(k_l \to k_{l+1}) = V_{k_l,k_{l+1}}/(E_\alpha - E_{k_l}^0)$. Then, defining the contribution of a path s from k_0 to k_q as

$$f_\alpha^s(k_0 \to k_q) = \prod_{l=0}^{q-1} D_\alpha(k_l \to k_{l+1}), \tag{5}$$

the expansion of $C_{\alpha j}$ on the right hand side of Eq. (4) can be written in the form

$$C_{\alpha j} = \sum_{|i\rangle \in S_\alpha} A_\alpha(j \to i) C_{\alpha i}, \tag{6}$$

where

$$A_\alpha(j \to i) = \left\langle j \left| \sum_{n=1}^{\infty} T_\alpha^n \right| i \right\rangle = \sum_s f_\alpha^s(j \to i), \tag{7}$$

with s denoting possible paths from j to i.

Substituting Eq. (6) into the Schrödinger equation

$$\sum_k H_{ik} C_{\alpha k} = E_\alpha C_{\alpha i}, \tag{8}$$

we have an eigenequation for the components $C_{\alpha i}$ of $|i\rangle$ in S_α,

$$\sum_{|i'\rangle \in S_\alpha} \tilde{H}_{ii'} C_{\alpha i'} = E_\alpha C_{\alpha i}, \tag{9}$$

where the *reduced Hamiltonian matrix* $\tilde{H} = \tilde{H}^0 + \tilde{V}$ is defined by

$$\tilde{H}_{ii}^0 = E_i^0 + \sum_{|j\rangle \in \overline{S}_\alpha} V_{ij} A_\alpha(j \to i), \tag{10}$$

$$\tilde{V}_{ii'} = V_{ii'} + \sum_{|j\rangle \in \overline{S}_\alpha} V_{ij} A_\alpha(j \to i'). \tag{11}$$

That is, the components $C_{\alpha i}$ compose an eigenfunction of the reduced Hamiltonian matrix $\tilde{H}$ with the same eigenenergy. The two summations in Eqs. (10) and (11) can be expressed in simple forms as $(E_\alpha - E_i^0)A_\alpha(i \to i)$ and $(E_\alpha - E_i^0)A_\alpha(i \to i')$, respectively, where $A_\alpha(i \to i')$ is defined by

$$A_\alpha(i \to i') = \sum_s f_\alpha^s(i \to i'). \tag{12}$$

The dimension of $\tilde{H}$ is the number of states in the set S_α. Note that $A_\alpha(j \to i)$ is a function of E_α. The reduced Hamiltonian matrices are Hermitian, since for a path s of $j_1 \to j_2 \cdots \to j_q \to i'$,

$$V_{ij_1} f_\alpha^s(j_1 \to i') = V_{ij_1} \frac{V_{j_1 j_2}}{E_\alpha - E_{j_1}^0} \cdots \frac{V_{j_q i'}}{E_\alpha - E_{j_q}^0}$$

$$= (V_{i' j_q} f_\alpha^{s'}(j_q \to i))^*, \tag{13}$$

where s' denotes the path $j_q \to \cdots \to j_1 \to i$.

The matrix elements of $\tilde{H}$ are closely related to $A_\alpha(j \to i)$. When the Hamiltonian H has a band structure in the H_0 representation, with zero coupling outside the band, $A_\alpha(j \to i)$ usually has an exponential-type decay with increase of the smallest number of paces from j to i. To show this, we expand the state $Q_{\overline{S}_\alpha}V|i\rangle$ in $|\nu_\alpha\rangle$, the (right) eigenvectors of the operator

$$U_\alpha \equiv Q_{\overline{S}_\alpha} V \frac{1}{E_\alpha - H^0} Q_{\overline{S}_\alpha} \tag{14}$$

with eigenvalues $u_{\alpha\nu}$, which gives $Q_{\overline{S}_\alpha}V|i\rangle = \Sigma_\nu h_\nu^i|\nu_\alpha\rangle$. Then we have

$$A_\alpha(j\to i)=\frac{1}{E_\alpha-E_j^0}\sum_\nu\left[\frac{h_\nu^i}{1-u_{\alpha\nu}}\langle j|\nu_\alpha\rangle\right](u_{\alpha\nu})^{m-1}, \tag{15}$$

where m is the smallest positive integer for $\langle j|(Q_{S_\alpha}^- V)^m|i\rangle$ not equal to zero, i.e., the smallest number of paces from j to i. As shown in Ref. [11], $|u_{\alpha\nu}|<1$, except for some very occasional cases, namely, $\langle\nu_\alpha|Q_{S_\alpha}^- V|\alpha\rangle=0$.

III. RELATION BETWEEN LOCALIZATION IN THE WBRM MODEL AND IN A BRM MODEL

A. The WBRM model in intermediate basis states

The Hamiltonian matrix of the WBRM model studied in this paper is chosen of the form

$$H_{cd}=(H_0^{\rm w}+\lambda V^{\rm w})_{cd}=E_c^{0{\rm w}}\delta_{cd}+\lambda v_{cd}^{\rm w} \tag{16}$$

$(c,d=1,\ldots,N)$, where $E_c^{0{\rm w}}=c$ are eigenenergies of $H_0^{\rm w}$. The off-diagonal matrix elements $v_{cd}^{\rm w}=v_{dc}^{\rm w}$ are random numbers with Gaussian distribution for $1\leqslant|c-d|\leqslant b$ $[\langle v_{cd}^{\rm w}\rangle=0$ and $\langle(v_{cd}^{\rm w})^2\rangle=1]$ and are zero otherwise. Here b is the bandwidth of the Hamiltonian matrix and N is its dimension. The eigenstates of $H_0^{\rm w}$, denoted by $|c\rangle$, are taken as the original basis states. The eigenstates of H are also denoted by $|\alpha\rangle$.

For this model, the *NPT region* of a perturbed state $|\alpha\rangle$ in the basis states $|c\rangle$ is defined as the smallest set

$$S_\alpha=\{|c_1\rangle,|c_1+1\rangle,\ldots,|c_2\rangle\} \tag{17}$$

satisfying the condition (3), with the rest of the states $|c\rangle$ defined as the *PT region* of $|\alpha\rangle$. To avoid confusion with the PT and NPT regions in intermediate basis states which will be introduced below, we denote the above PT and NPT regions as the PT_c and NPT_c regions, respectively. Correspondingly, the state $|\alpha\rangle$ and its components in $|c\rangle$ are divided into NPT_c and PT_c parts, respectively. For a given value of b, the eigenfunctions of $|\alpha\rangle$ in $|c\rangle$ are localized, when the perturbation parameter λ and dimension N are large enough (see the detailed condition given in Ref. [2]), e.g., when $\lambda=25, b=4$, and $N=500$, which are the parameters taken in our numerical calculation and give $(c_2-c_1)\gg b$. A direct application of the results given in Sec. II does not give any clue to the explanation of the localization in the model, since $\tilde{H}_{cd}=H_{cd}$ for labels c and d in the region $[c_1+b,c_2-b]$.

The method of the reduced Hamiltonian matrix can be improved by employing intermediate basis states. To construct a set of intermediate basis states , we first choose a positive integer n_i which is much smaller than N and subdivide the Hilbert space into a series of subspaces, denoted by $\mathcal{G}_l$ $(l=1,2,\ldots,l_m)$, where $\mathcal{G}_l$ is spanned by states $|c\rangle$ of $c=n_i(l-1)+1,n_i(l-1)+2,\ldots,n_i l$. [For l_m, $c=n_i(l_m-1)+1,\ldots,N$.] Second, we calculate the eigenstates of the Hamiltonian in each of the subspaces $\mathcal{G}_l$, denoted by $|k\rangle$ $[k=n_i(l-1)+1,n_i(l-1)+2,\ldots n_i l$ for $\mathcal{G}_l]$. The states $|k\rangle$ with $k=1,2,\ldots,N$ are taken as *intermediate basis states*. For convenience in using the results in Sec. II, the diagonal and off-diagonal parts of the matrix of H in the intermediate basis states are denoted by H_0 and V, with elements $E_k^0=\langle k|H|k\rangle$ and $V_{kk'}=\langle k|H|k'\rangle$, respectively. In this paper, with the parameters $\lambda=25$ and $b=4$, except for the case of $n_i=1$ in which $|k\rangle=|c\rangle$, we are interested in $n_i\geqslant b$ only, the reason for which will be clear from the numerical results presented below. In this case, for two states $|k\rangle$ and $|k'\rangle$ in two subspaces $\mathcal{G}_{l_k}$ and $\mathcal{G}_{l_{k'}}$, respectively, $V_{kk'}$ is nonzero only when $\Delta l=|l_k-l_{k'}|=1$; therefore, the matrix $H_{kk'}$ has a band structure as well. The number of paces of the shortest path from k to k' with respect to $V_{kk'}$ is just Δl, when $\Delta l\neq0$. As a result, $\tilde{V}_{ii'}$ in Eq. (11) has an exponential-type decay with increasing $\Delta l=|l_i-l_{i'}|$, when $\Delta l>2$ [see Eq. (15)].

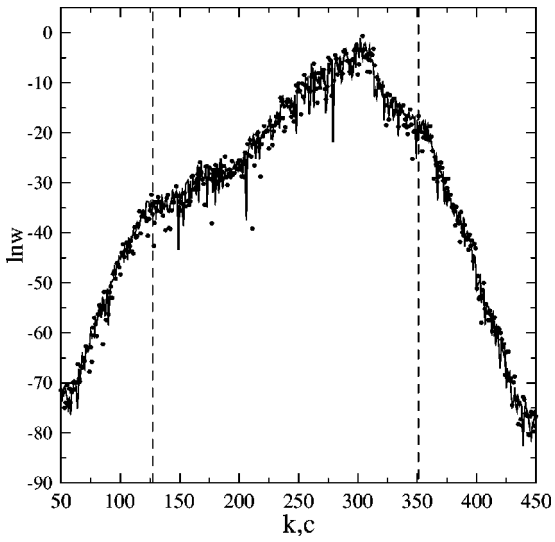

FIG. 1. Shape of the eigenfunction of an eigenstate $|\alpha\rangle$ in the original basis states $|c\rangle$ (solid line) and its counterpart in intermediate basis states $|k\rangle$ of $n_i=7$ (dots), when $b=4$ and $\lambda=25$. $w=|\langle x|\alpha\rangle|^2$, with x being c or k. The two vertical dashed lines indicate the positions of c_1 and c_2, respectively, of the NPT_c region of $|\alpha\rangle$.

When the value of n_i is obviously smaller than the localization length of $|\alpha\rangle$ in the original basis states $|c\rangle$, the change of basis states will have no influence on whether the eigenfunctions are localized (see Fig. 1 for the example of $n_i=7$). In the case of the parameters in our calculation, the average localization length of the eigenfunctions of the matrices in Eq. (16), calculated by information entropy, has been found to be 33.7. Note that E_k^0 are not in energy order. In the calculation of the NPT region of $|\alpha\rangle$ in intermediate basis states, denoted as the NPT_k region, we relabel $|k\rangle$ in energy order, denoted by $|k^e\rangle$, and use k^e instead of c in Eq. (17). The sizes of the NPT_k regions thus obtained, denoted by $N_\alpha=k_2^e-k_1^e+1$, have been found to decrease rapidly, when n_i increases from 1 to some value n_c. Figure 2(a) shows the average behavior of N_α, where $\langle n_c\rangle\approx7$. A major reason for the reduction of NPT regions is that, for each subspace $\mathcal{G}_l$, the region of magnitude occupied by E_k^0 enlarges with increasing n_i (see Fig. 3 for $n_i=7$). The average coupling strength $v=\sqrt{\langle V_{kk'}^2\rangle}$, with averaging taken over

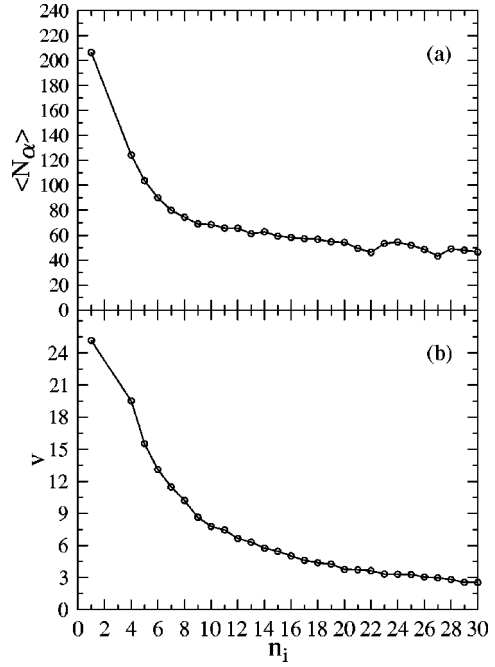

FIG. 2. (a) Values of $\langle N_\alpha \rangle$, the average size of NPT_k regions of $|\alpha\rangle$, as a function of n_i. (b) Variation of the average coupling strength $v=\sqrt{\langle V_{kk'}^2 \rangle}$ with n_i.

nonzero $V_{kk'}$, also decreases with increasing n_i [Fig. 2(b)], which is another reason of for reduction of NPT regions.

Numerically, a feature of E_k^0 has been found related to some properties of the NPT_c regions of states $|\alpha\rangle$. In the case of the original basis states ($n_i=1$), the points (c,E_c^0) lie in a straight line in the c-E^0 plane. With increasing n_i, the rough boundary of the region occupied by the points (k,E_k^0) expands in the direction perpendicular to the straight line. However, the expansion of the rough boundary has been found to slow down obviously, when n_i reaches some value depending on b and λ, which is equal to 7 for the parameters in our calculation (Fig. 3). In fact, almost the same rough boundaries have been observed when $n_i=7$ and when $n_i=20$. An interesting feature shown in Fig. 3 is that, when one draws a horizontal dotted line meeting the E^0 axis at $E^0=E_\alpha$ of a state $|\alpha\rangle$ and two vertical dash-dotted lines meeting the k axis at $k=c_1$ and c_2, respectively, the crossing points of the three lines are quite close to the rough boundary of the region of (k,E_k^0). This property of E_k^0 should be useful in the approximate calculation of NPT_c regions.

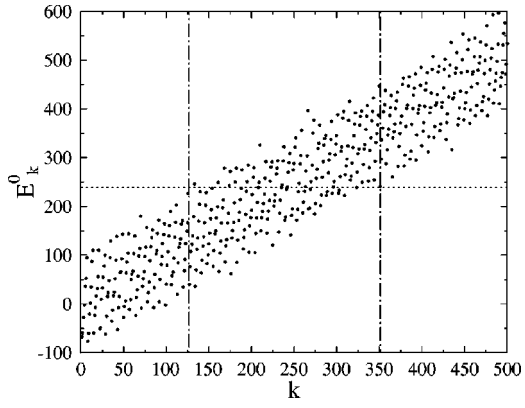

FIG. 3. Values of $E_k^0=\langle k|H^{\mathrm{w}}|k\rangle$ obtained with $n_i=7$. The horizontal dotted straight line indicates the position of E_α, the energy of a state $|\alpha\rangle$, on the vertical axis. Vertical dash-dotted straight lines indicate positions of the values of c_1 and c_2, the boundaries of the NPT_c region of $|\alpha\rangle$, on the horizontal axis.

B. Reduced Hamiltonian matrices in intermediate basis states

In this subsection, we discuss the properties of reduced Hamiltonian matrices in intermediate basis states. In our numerical calculation, we choose $n_i=7$, because of its properties discussed in the previous subsection. Since matrices of H in the label k have a simpler coupling structure than the ones in the energy-ordered label k^e, we return to the label k when the NPT_k regions of states $|\alpha\rangle$ have been calculated.

For the sake of convenience, we use $|i\rangle$ to denote states $|k\rangle$ in the NPT_k region of $|\alpha\rangle$ and $|j\rangle$ to denote those in the PT_k region. Equations (10) and (11) show that both $\tilde{H}_{ii}^0$ and $\tilde{V}_{ii'}$ associated with a state $|\alpha\rangle$ are composed of two parts with different origins. One is the corresponding elements of H, the other is the contribution from the PT_k region. To show this more clearly, we introduce

$$x_{ii'}=\sum_j V_{ij}A_\alpha(j\rightarrow i'), \tag{18}$$

$$y_i=\sum_j V_{ij}A_\alpha(j\rightarrow i). \tag{19}$$

Unperturbed energies E_i^0 in the NPT_k region of a state $|\alpha\rangle$ are those that are close to E_α, e.g., the 80 points closest to the dotted line in Fig. 3. For perturbed states $|\alpha\rangle$ in the middle of the energy region, the upper and lower bounds of E_i^0 are on average symmetric with respect to E_α; as a result, the average of $(E_i^0-E_\alpha)$ is zero. In studying statistical properties of the reduced Hamiltonian matrices associated with such perturbed states, it would be better to shift their diagonal parts $\tilde{H}_{ii'}^0$ to

$$e_i=e_i^0+y_i, \tag{20}$$

where $e_i^0=E_i^0-E_\alpha$.

As discussed in the previous subsection, $\tilde{V}_{ii'}$ has an exponential-type decay when $|l_i-l_{i'}|>2$. As a result, the reduced Hamiltonian matrices should, on average, have a band structure with an effective bandwidth b_e, which is approximately $(5N_n-1)/2$, where N_n is the average number of states $|i\rangle$ in a subspace $\mathcal{G}_l$, found to be about 2.06 in our numerical calculation, giving $b_e\approx 4.65$. This prediction of b_e is in agreement with that obtained from a direct calculation of $u(\Delta i)=\sqrt{\langle \tilde{V}_{ii'}^2 \rangle}$, where $\Delta i=(i-i')$, which is shown in Fig. 4, with averaging taken over i of 550 reduced Hamiltonian matrices coming from 50 matrices H_{cd} of different realizations of random numbers. For comparison, the values of $u_e=\sqrt{\langle e_i^2 \rangle}$ are also presented in Fig. 4, at the position of

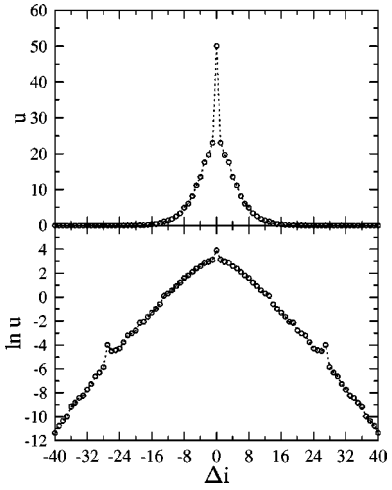

FIG. 4. Values of $u(\Delta i)=\sqrt{\langle \tilde{V}_{ii'}^2 \rangle}$ and $\ln u$, showing the band-like structure of the off-diagonal elements of reduced Hamiltonian matrices, where the average is taken over i with $i'=i-\Delta i$. For comparison, the values of $u_e=\sqrt{\langle e_i^2 \rangle}$ and $\ln u_e$ for the diagonal elements are shown at the positions of $\Delta i=0$.

$\Delta i=0$, which is larger than $2u(\Delta i)$ of $\Delta i=\pm 1$. In the calculation of the elements of the reduced Hamiltonian matrices, the expansion of $A_\alpha(j\rightarrow i)$ in Eq. (7) was truncated at the first n satisfying $|\langle j|T_\alpha^n|i\rangle| \leqslant 10^{-14}$.

Now let us discuss the distributions of elements of the reduced Hamiltonian matrices. Due to the random signs of $V_{kk'}$, y_i also has random signs, with zero mean. Figure 5(a) shows that the central part of the distribution of e_i can be fitted well by both a Gaussian distribution and a stable Lévy distribution

$$L(p)=\frac{1}{\pi}\int_0^{+\infty} \exp(-\gamma q^\alpha)\cos(qp)dq, \tag{21}$$

for Lévy flights with infinite variance (see, e.g., Refs. [19–21]). The fitting of the Lévy distribution is in fact a little better than that of the Gaussian distribution. In the tail region, the distribution $f(e)$ is obviously closer to the Lévy distribution than to the Gaussian [Fig. 6(a)]. Since $\alpha=1.7$ for the best fitting Lévy distribution, the distribution $f(e)$ is far from the Lorentzian distribution, which is a special case of the Lévy distribution with $\alpha=1$.

The distributions of the two constituents of e_i in Eq. (20) have also been studied. The distribution of e_i^0 is close to neither a Gaussian distribution nor a Lévy distribution. In fact, its central part has a platform [Fig. 5(b)] and its long tails decrease faster than a Gaussian distribution. These two properties of $f(e^0)$ are simply due to the requirement of the GBWPT that E_i^0 in the NPT$_k$ region of $|\alpha\rangle$ are those E_k^0 which are close to E_α. An estimation of the width of the central part of $f(e^0)$ is given in the Appendix. We should mention that, although the mean value of e_i^0 is zero, there is still some small remnant of the influence of the increasing diagonal elements of H_0^{W} in the original basis, for example, in Fig. 3 most of the points close to the left vertical dash-dotted line are below the horizontal dotted line, but those close to

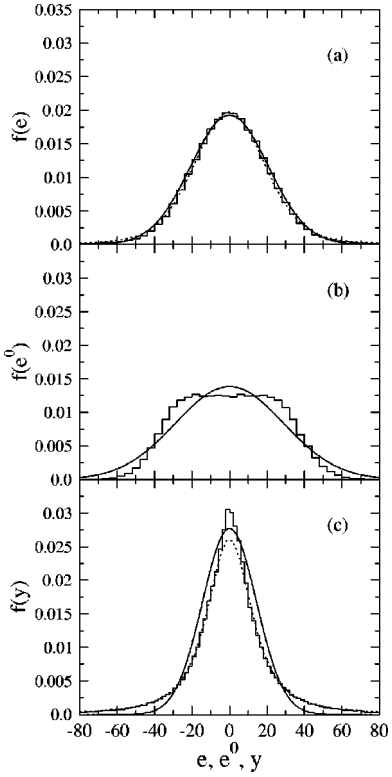

FIG. 5. (a) The histogram is the distribution of diagonal elements of the reduced Hamiltonian matrices, e_i, calculated from 5000 reduced Hamiltonian matrices belonging to 500 realizations of the original random matrices. The dotted curve is the best fitting Lévy distribution, with $\alpha=1.7$ and $\gamma=94.1$. The solid curve is the best fitting Gaussian distribution. (b) Same as in (a), for the distribution of e_i^0, without fitting of the Lévy distribution. (c) Same as in (a), for the distribution of y_i, with $\alpha=1.22$ and $\gamma=18.8$ for the best fitting Lévy distribution.

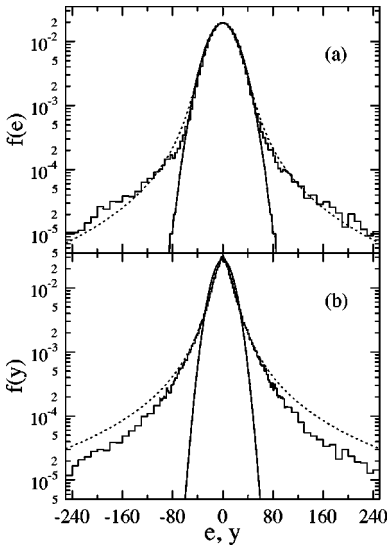

FIG. 6. (a) Same as in Fig. 5(a), on a logarithmic scale. (b) Same as in Fig. 5(c), on a logarithmic scale.

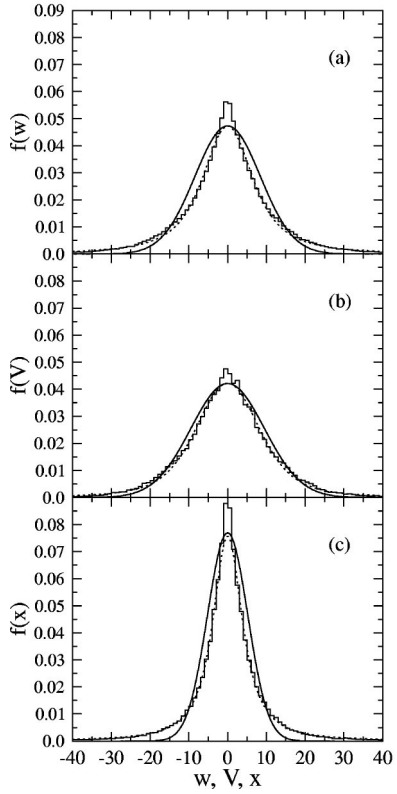

FIG. 7. (a) Same as in Fig. 5(a), for the distribution of $w=\tilde{V}_{ii'}$ within the effective bandwidth of reduced Hamiltonian matrices, with $\alpha=1.21$ and $\gamma=9.33$ for the best fitting Lévy distribution. (b) Same as in (a), for the distribution of nonzero $V_{ii'}$, with $\alpha=1.49$ and $\gamma=17.3$. (c) Same as in (a), for the distribution of $x_{ii'}$ with $|l_i-l_{i'}|=0$. For the best fitting Lévy distribution, $\alpha=1.11$ and $\gamma=4.7$.

the right dash-dotted line are above the horizontal dotted line. The distribution of y_i is shown in Fig. 5(c). Its central part is quite close to a Lévy distribution with $\alpha=1.22$, except in the region of small y. Consistently with the fact that $f(y)$ is higher than the best fitting Lévy distribution in the top region, its tails, which also have a power-law decay feature, are lower than the ones of the Lévy distribution [Fig. 6(b)].

In a statistical study of off-diagonal elements of reduced Hamiltonian matrices, one should distinguish between those within the effective bandwidth and those outside. The distribution of $\tilde{V}_{ii'}$ within the effective bandwidth, namely, for which $\Delta l=|l_i-l_{i'}|\leqslant 2$, is shown in Fig. 7(a). Again, it is close to the best fitting Lévy distribution in the central part, except in the high peak region, but cannot be fitted well by the Gaussian distribution. A similar relation to the Lévy distribution has also been found for the distributions of nonzero $V_{ii'}$ [Fig. 7(b)] and of $x_{ii'}$ with different Δl. In fact, the central parts of $f(x)$ (except in the high peak regions) have been found to be fitted quite well by the Lévy distribution, e.g., see Fig. 7(c) for $\Delta l=0$. The width of the distribution $f(x)$ decreases with increasing Δl, consistent with the feature of $u(\Delta i)$ shown in Fig. 4.

The reduced Hamiltonian matrices discussed above suggest a BRM model with an effective bandwidth b_e, which has statistical properties more complicated than the standard BRM model. Although a fraction of the diagonal elements of the reduced Hamiltonian matrices, namely, the ones close to the two edges of the matrices, are not completely random, diagonal elements in the BRM model suggested here are set random. It is reasonable to expect that the small difference in diagonal elements does not affect whether eigenfunctions of the matrices are localized.

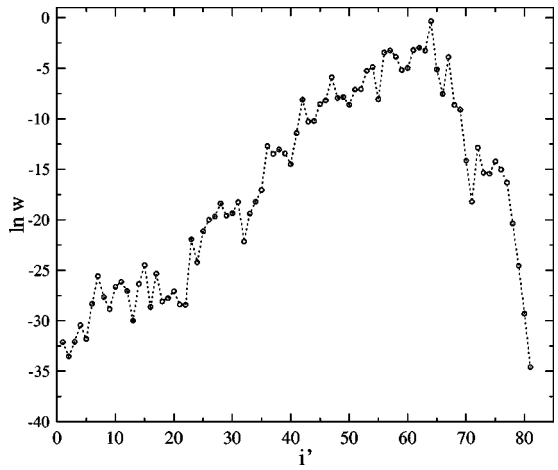

FIG. 8. Shape of an eigenfunction of a reduced Hamiltonian matrix, which is the NPT_k part of the eigenfunction shown in Fig. 1, with respect to a label i' shifted from i.

In the BRM model suggested here, u_e, the root mean square (rms) of the diagonal elements, is different from the rms of the off-diagonal elements within the band, denoted by u_{off}. Such a difference is a feature of the SBRM, which is the sum of a random diagonal matrix and a conventional BRM. The localization length in the SBRM model, denoted by l_{sb}, can be fitted well by the expression [18]

$$l_{sb}=1.6(b+0.5)/\ln[1+2.5(1.25W_b^2+1)/b], \qquad (22)$$

where b is the bandwidth of the SBRM and $W_b=\sqrt{(u_e/u_{\mathrm{off}})^2-1}/\sqrt{2b+1}$. Using the parameters of the reduced Hamiltonian matrices $b_e\approx 4.65$ and $u_e/u_{\mathrm{off}}\approx 2.8$, we have $l_{sb}\approx 12.0$. Noticing that the average dimension of the reduced Hamiltonian matrices is approximately 80, the SBRM has localized eigenfunctions when it has the same parameters as the BRM suggested here. Since the main difference between the SBRM model and the BRM suggested here lies in the types of distributions of matrix elements in them, it is reasonable to expect that eigenfunctions in the BRM model suggested here will be localized as well. Numerically, the eigenfunctions of the reduced Hamiltonian matrices have indeed been found localized; see Fig. 8 for an example, where the values of the label i have been shifted to $i'=1,2,\ldots,N_\alpha$, with order unchanged, for the sake of clearness in plotting. The similarity between the rough shape of the eigenfunction show in Fig. 8 and that of the NPT_c part of the original eigenfunction in Fig. 1 is quite obvious.

Finally, we show that, if the NPT_k part of a state $|\alpha\rangle$, namely, the components $C_{\alpha i}$, form a localized eigenfunction

of a reduced Hamiltonian matrix, the eigenfunction of $|\alpha\rangle$ in the original basis states $|c\rangle$ must be localized as well, when $n_i \ll N$. In fact, since the components $C_{\alpha j}$ in the PT_k part of $|\alpha\rangle$ can be expressed in terms of the components $C_{\alpha i}$ [Eq. (6)] and, due to the band structure of the Hamiltonian matrix $H_{kk'}$, $A_\alpha(j \to i)$ has an exponential-type decay with increasing $|l_j - l_i|$ [Eq. (15)], the eigenfunction of $|\alpha\rangle$ in the intermediate basis states $|k\rangle$ must be localized as well. There is no need to discuss the case of n_i being close to or larger than the localization length of $|\alpha\rangle$ in $|c\rangle$, which means that the eigenfunction is localized. For the other case, as discussed in Sec. III A, localization of the eigenfunction of $|\alpha\rangle$ in the original basis states $|c\rangle$ would follow; in particular, when n_i is obviously smaller than the localization length of the eigenfunction of $|\alpha\rangle$ in $|c\rangle$, the NPT part of $|\alpha\rangle$ in $|c\rangle$ should be localized as well.

IV. CONCLUSIONS AND DISCUSSION

In this paper, we have shown that localization in the Wigner band random matrix model can be related to localization of eigenfunctions of the corresponding reduced Hamiltonian matrices. First, for an arbitrary Hamiltonian composed of an unperturbed Hamiltonian and a perturbation, making use of a generalization of Brillouin-Wigner perturbation theory, it has been shown that a reduced Hamiltonian matrix can be introduced for each perturbed state, which has an eigenfunction sharing the same components as the nonperturbative part of the perturbed state in the representation of the unperturbed Hamiltonian. The reduced Hamiltonian matrices introduced here may be unsuitable to the calculation of exact eigenfunctions and eigenenergies, but are useful in the study of properties of eigenfunctions such as localization. Secondly, intermediate basis states have been used to make the method of reduced Hamiltonian matrices more suitable to the study of localization in the WBRM model. It has been shown that eigenfunctions of the WBRM model should be localized, if eigenfunctions of the corresponding reduced Hamiltonian matrices in intermediate basis states are localized.

Numerically, the reduced Hamiltonian matrices have been found related to a BRM model with random diagonal elements, which is close to a superimposed BRM model. The main difference between the two BRM models rests in the distribution forms of the matrix elements. It has been found that parameters of the BRM suggested here lie in the localization regime of the SBRM model. Eigenfunctions in the BRM suggested here have indeed been numerically found to be localized.

The distributions of the elements of reduced Hamiltonian matrices have been found to be close to the Lévy distribution numerically (except in the high top regions for off-diagonal elements). Presently, there is no analytical explanation for the closeness. However, a possible relationship would not be strange, since $A_\alpha(j \to i)$ are composed of factors of ratios of $V_{kk'}$ and $(E_\alpha - E_k^0)$. As is know, when a distribution of ratios is of interest, one may meet power-law decaying tails [22,23], which is a specific feature of the Lévy distribution. In fact, it is possible for a distribution of ratios to be very close to (even exactly) a Lorentzian distribution, which is a special case of the Lévy distribution, in both the central part and the tail region [24]. The reason is still unclear for the deviations of some of the distributions investigated here from their best fitting Lévy distributions in the top regions. One possibility is that the definition of the NPT parts of the eigenfunctions used here is not the best one. Indeed, there is no problem in using the definition here in the investigation of the structure of eigenfunctions [11], but distributions of ratios are more sensitive to the parts of the eigenfunctions considered than is the structure of the eigenfunctions.

When intermediate basis states are used, the sizes of the NPT parts of the eigenfunctions can be reduced considerably, which makes the GBWPT more effective. A shortcoming of this approach is that it is generally impossible to write down the elements of Hamiltonian matrices in intermediate basis states analytically. Usually this causes no problem in numerical calculations, since the sizes of the submatrices for calculating intermediate basis states are small. Reduced Hamiltonian matrices may also be useful in improving the method of calculating approximate eigenenergies and eigenfunctions of large matrices by diagonalization of some relatively small matrices [25–27]. A difficulty met in this direction is that different original eigenfunctions correspond to different reduced Hamiltonian matrices. This problem may be partly solved, if in some models the reduced Hamiltonian matrices associated with close energies have similar elements.

ACKNOWLEDGMENT

Partial support from the Academic Research Fund of NUS is gratefully acknowledged.

APPENDIX: ESTIMATION OF THE WIDTH OF THE CENTRAL PART OF $F(E^0)$

Note that the half-width of the central part of $f(e^0)$ is approximately equal to the average distance between the upper and lower bounds of E_i^0 in NPT_k regions of the perturbed states $|\alpha\rangle$, denoted by δe, $\delta e = \langle E_{k_2^e}^0 - E_{k_1^e}^0 \rangle$. In the general case that $|u_{\alpha\nu}| < 1$, the left hand side of Eq. (3) is either zero or infinity. For the purpose of an estimation of the left hand side of Eq. (3), one can consider

$$I_n = N_p \left(\frac{\overline{v}}{\langle \Delta E \rangle} \right)^n, \tag{A1}$$

where N_p is the effective number of paths involved, and $\overline{v}$ and $\langle \Delta E \rangle$ are the geometric means of nonzero coupling and of $|E_\alpha - E_j^0|$ in the paths, respectively. Suppose the average number of nonzero couplings of a state $|j\rangle$ to other states $|j'\rangle$ is b_c. An estimation of N_p gives

$$N_p \propto (\beta' b_c)^n, \tag{A2}$$

with β' being an undetermined parameter less than 1. Since $|E_\alpha - E_j^0|$ is usually larger than $\delta e/2$, we write $\langle \Delta E \rangle$ as $\beta'' \delta e/2$, with $\beta'' > 1$ undetermined. Taking a parameter

$\beta=2\beta'/\beta''$, we have an estimation for the average size of the NPT regions,

$$\delta e \approx \beta b_c \overline{v}, \tag{A3}$$

by using the condition $0<\lim_{n\to\infty} I_n<\infty$.

The above arguments leading to Eq. (A3) hold generally for Hamiltonian matrices with band structure. In cases where the nonzero off-diagonal elements are random, the values of β should be the same or close. Therefore, the numerical results given in Ref. [11] for the WBRM model in the original basis states can be used to calculate β, which gives $\beta \approx 0.7$, with $\delta e \approx 140$ when $\overline{v}=10$ and $b_c=2b=20$. Here the root mean square of nonzero off-diagonal elements $V_{cc'}$ is used for $\overline{v}$, with the difference absorbed in β. For the Hamiltonian matrices of the WBRM model in intermediate basis states discussed in this paper, $b_c=2(n_i-N_n)\approx 9.9$, $v \approx 11.5$; as a result, $\delta e \approx 76.2$, close to the half-width of $f(e^0)$ shown in Fig. 5(b).

[1] G. Casati, B. V. Chirikov, J. Ford, and F. M. Izrailev, in *Stochastic Behavior in Classical and Quantum Hamiltonian Systems*, Lecture Notes in Physics Vol. 93 (Springer-Verlog, Berlin, 1979), p. 334.

[2] G. Casati, B.V. Chirikov, I. Guarneri, and F.M. Izrailev, Phys. Lett. A **223**, 430 (1996).

[3] F. Borgonovi, G. Casati, and B. Li, Phys. Rev. Lett. **77**, 4744 (1996).

[4] K. Frahm and D.L. Shepelyansky, Phys. Rev. Lett. **78**, 1440 (1997); **79**, 1833 (1997).

[5] F. Borgonovi, Phys. Rev. Lett. **80**, 4653 (1998).

[6] G. Casati and T. Prosen, Phys. Rev. E **59**, R2516 (1999).

[7] E. Wigner, Ann. Math. **62**, 548 (1955); **65**, 203 (1957).

[8] V.V. Flambaum, A.A. Gribakina, G.F. Gribakin, and M.G. Kozlov, Phys. Rev. A **50**, 267 (1994).

[9] Y.V. Fyodorov, O.A. Chubykalo, F.M. Izrailev, and G. Casati, Phys. Rev. Lett., **76**, 1603 (1996).

[10] Wen-ge Wang, F.M. Izrailev, and G. Casati, Phys. Rev. E **57**, 323 (1998).

[11] Wen-ge Wang, Phys. Rev. E **61**, 952 (2000); Commun. Theor. Phys. **35**, 143 (2001).

[12] S. Fishman, D.R. Grempel, and R.E. Prange, Phys. Rev. Lett. **49**, 509 (1982); D.R. Grempel, R.E. Prange, and S. Fishman, Phys. Rev. A **29**, 1639 (1984).

[13] G. Casati, L. Molinari, and F. Izrailev, Phys. Rev. Lett. **64**, 1851 (1990).

[14] Y.V. Fyodorov and A.D. Mirlin, Int. J. Mod. Phys. B **8**, 3795 (1994).

[15] F.M. Izrailev, Chaos, Solitons Fractals **5**, 1219 (1995).

[16] T. Guhr, A. Müller-Groeling, and H.A. Weidenmüller, Phys. Rep. **299**, 189 (1998).

[17] F. Haake, *Quantum Signatures of Chaos*, 2nd ed. (Springer-Verlag, Berlin, 2001).

[18] D.L. Shepelyansky, Phys. Rev. Lett. **73**, 2607 (1994).

[19] R.N. Mantegna and H.E. Stanley, Phys. Rev. Lett. **73**, 2946 (1994).

[20] *Lévy Flights and related Topics in Physics*, edited by M. Shlesinger, G. Zaslavsky, and U. Frisch (Springer-Verlag, Berlin, 1995).

[21] K. Umeno, Phys. Rev. E **58**, 2644 (1998).

[22] F.J. Dyson, Phys. Rev. **92**, 1331 (1953).

[23] C. Barnes and J.M. Luck, J. Phys. A **23**, 1717 (1990); J. M. Luck, *Systèmes Désordonnés Unidimensionnels* (Collection Aléa Saclay, Paris, 1992).

[24] B. Hu, B. Li, and W. Wang, Europhys. Lett. **50**, 300 (2000); Wang Wen-ge, Commun. Theor. Phys. **36**, 271 (2001).

[25] M. Horoi, B.A. Brown, and V. Zelevinsky, Phys. Rev. C **50**, R2274 (1994).

[26] M. Horoi, A. Volya, and V. Zelevinsky, Phys. Rev. Lett. **82**, 2064 (1999).

[27] Wen-ge Wang, Phys. Rev. E **63**, 036215 (2001).